AIAA 81-2015R

# Accuracy and Stability of Finite Element Schemes for the Duct Transmission Problem

R. J. Astley,* N. J. Walkington,† and W. Eversman‡
*University of Missouri-Rolla, Rolla, Missouri*

**A one-dimensional numerical model is used to investigate the characteristics of finite element computational schemes for linearized acoustical transmission in ducts with flow. Primitive variables and coupled first-order equations are used. The relative performances of Lagrangian and Hermitian elements with Galerkin and residual least squares formulations are assessed. Results of the numerical study are shown to correlate with the characteristics of analytic solutions for the equivalent regular grid difference equations. Galerkin solutions are shown to introduce spurious nonphysical modes which must be eliminated by careful attention to the local resolution requirements of the finite-element mesh. Residual least squares formulations do not introduce spurious numerical modes but result in significant numerical damping. This is particularly severe if Lagrangian elements are used.**

## Introduction

THE finite element method (FEM) has been applied to the problem of acoustic transmission in nonuniform ducts with increasing frequency in recent years.[1-12] The numerical solution of this problem is of practical interest in the context of noise attenuation in the ducted regions of turbofan aircraft engines with the FEM approach offering as one of its attractive general features the potential for multipurpose programs capable of handling arbitrary geometries and lining configurations.

All FEM formulations of the problem to date have treated the "steady" linear case with implicit harmonic time dependence of all variables. With the exception of the authors' own treatment of the uniform duct eigenvalue problem,[10] the space discretization in all formulations has comprised linear or quadratic Lagrangian ($C_0$ continuous) elements. Most FEM analyses are based on residual schemes, although in the case with no mean flow a variational statement of the problem is possible.[1-3,9] The residual formulations used are generally variants of the Galerkin process although the method of residual least squares has also been proposed as a computationally attractive alternative.[8,12] When no mean flow is present or when the mean flow is irrotational the problem may be formulated in terms of a single dependent variable (pressure or velocity potential). This approach yields a second-order equation of modified Helmholtz form. For the case of a rotational mean flow, as in the inlet region of an aircraft engine, the use of a velocity potential to describe the acoustical field is no longer appropriate and the problem must be formulated in terms of coupled first-order equations in the primitive variables (pressure and velocity). This is the approach that the authors have adopted in all previous work[4,7,10-12] and it is the efficiency of schemes based on this type of formulation which is investigated in this paper.

Comparison of existing FEM schemes of the type just described with alternative numerical methods have demonstrated their overall utility[4,12] as have recent comparisons with experimental data.[13] Large matrix orders, however, are involved in FEM solutions for the high frequencies and Mach numbers present in realistic turbofan inlet configurations. Therefore, it is appropriate at this stage in the development of FEM models and prior to their application either in practical design or in more computationally demanding nonlinear regimes, that a careful study of possible improvements to the efficiency and stability of existing FEM schemes should be undertaken. An investigation of this sort, including both analytical and numerical studies, is reported in this paper.

One motivation for the present investigation lay in an explanation of the behavior exhibited by some solutions of the authors own two-dimensional/axisymmetric formulation of Ref. 12. Of particular concern was the apparent inaccuracy of the residual least squares (RLS) formulation when compared with the equivalent Galerkin schemes. The RLS method had the otherwise attractive feature of producing a self-adjoint stiffness matrix. It was therefore of considerable interest to establish whether its poor performance was due to the element type used or whether a more fundamental problem was involved. The behavior of an analogous scheme with Hermitian ($C_1$ continuous) elements was of particular interest to the authors both because a discretization of this sort had resulted in significantly improved accuracy in their treatment of the uniform duct eigenvalue problem[10] and because of evidence from related problems[14] that RLS formulations require higher orders of continuity than their Galerkin counterparts to compete effectively in terms of overall accuracy.

Another feature of concern in the two-dimensional results of Ref. 12 was the appearance at high frequencies and Mach numbers of resolution difficulties characterized by pressure and velocity fields with severe slope discontinuities at element boundaries. Qualitatively similar behavior is well documented in other areas of FEM applications[15] and is generally associated with the residual formulation used. For the current problem it was of interest to establish the effect both of element type and residual formulation on spatial instabilities of this sort.

With the resolution of the preceding questions in mind a simple one-dimensional model of the duct transmission problem was developed to evaluate the performances of various elements and residual schemes. Lagrangian and Hermitian elements were implemented with Galerkin and RLS minimization giving a total of four alternative formulations. The one-dimensional model itself incorporates all the significant features of the two-dimensional and axisymmetric formulations without involving the purely algebraic and computational difficulties associated with two-dimensional elements. The solution times for the one-dimensional models

Presented as Paper 81-2015 at the AIAA 7th Aeroacoustics Conference, Palo Alto, Calif., Oct. 5-7, 1981; submitted Oct. 26, 1981; revision received March 8, 1982. 

*Visiting Associate Professor, Mechanical and Aerospace Engineering Department. Member AIAA.

†Graduate Student, Mechanical and Aerospace Engineering Department.

‡Professor and Chairman, Mechanical and Aerospace Engineering Department. Member AIAA.

are typically two orders of magnitude smaller than those for the analogous two-dimensional or axisymmetric models and it was possible therefore to test the various formulations to the limits of their accuracy at modest computational cost. The trends already observed in the two-dimensional Lagrangian results of Ref. 12 are reflected clearly in the behavior of the one-dimensional models and there is little doubt that the conclusions reached from the current investigation may be applied confidently to the two- and three-dimensional cases. A description of the one-dimensional model and a review of the results obtained from it are presented in the first two sections of this paper.

An explanation of the general behavior of the various FEM schemes may also be found in an analysis of the resulting nodal difference equations which yield analytic solutions for the case of uniform ducts with regular grids. The form of these solutions is discussed in the final section of the paper.

## Problem Statement and Finite-Element Formulations

### Duct Geometry and Governing Equations

The geometry of the duct is shown in Fig. 1 and comprises a nonuniform segment of sectional area $A(x)$ terminated by uniform sections at $x=0$ and $x=L$. A steady mean flow is assumed within the duct and all dependent variables are nondimensionalized with respect to reference values $\rho_r$ and $c_r$ of density and sound speed, respectively. The nondimensionalization is detailed in Ref. 12. If a harmonically varying, plane, acoustical perturbation of frequency $\omega$ is then assumed, the axial velocity and density perturbation amplitudes $u$ and $\rho$ are given by the solution of the linearized momentum and continuity equations;

$$iku + U_0 \frac{du}{dx} + u\frac{dU_0}{dx} + \frac{dp_0}{dx}(\gamma-2)\frac{\rho}{\rho_0^2} + \frac{\gamma p_0}{\rho_0^2}\frac{d\rho}{dx} = 0 \quad (1)$$

and

$$ik\rho + \frac{1}{A}\frac{d}{dx}(AU_0\rho + A\rho_0 u) \quad (2)$$

The reduced frequency $k$ in the preceding equations is given by $k=\omega/c_r$ and the mean flow velocity, density, and pressure $U_0$, $\rho_0$, and $p_0$ are solutions of the one-dimensional nozzle equations for isentropic flow. Equations (1) and (2) are in fact a generalized form of Webster's horn equation with mean flow included and represent physically the case of acoustical transmission at a frequency below that for "cut on" of the first transverse mode.

### Boundary Conditions

At the ends of the nonuniformity the boundary conditions on $u$ and $\rho$ are formulated as modal expansions of the uniform duct eigensolutions. Accordingly, at $x=0$ and $x=1$ $\rho$ and $u$ are written

$$\begin{Bmatrix} u \\ \rho \end{Bmatrix} = \begin{bmatrix} c_0/\rho_0, & -c_0/\rho_0 \\ 1, & 1 \end{bmatrix} \begin{Bmatrix} a^+ e^{-ik^+x} \\ a^- e^{-ik^-x} \end{Bmatrix} \quad (3)$$

where $k^+$ and $k^-$, the axial wavenumbers of positively and negatively propagating modes, are given by

$$k^\pm = k/(U_0 \pm c_0) \quad (4)$$

In general the boundary conditions for the problem will consist of specified values of $a^+$ or $a^-$ at each end of the nonuniformity. For all the results presented in this paper it will be assumed that the coefficient $a^+$ is known at $x=0$ and that the coefficient $a^-$ is zero at $x=L$. This boundary condition simulates an anechoic termination at each end of the nonuniformity with a known incident mode at the left-hand end. The ability to impose modal boundary conditions of this sort is an important feature of the two-dimensional and axisymmetric formulations which was important to preserve in the one-dimensional model.

### Formation of the Trial Function

Initially a standard FEM discretization is implemented by subdividing the interval $0 \le x \le L$ into finite line elements. Trial functions $\tilde{u}$ and $\tilde{\rho}$ are then defined by

$$\tilde{u} = [N_g]\{u\} \text{ and } \tilde{\rho} = [N_g]\{\rho\} \quad (5)$$

where $\{N_g\}$ is a global shape matrix with components specified implicitly inside each element by the appropriate element shape functions. The components of $\{u\}$ and $\{\rho\}$ are suitably ordered nodal variables for velocity and density and constitute the degrees of freedom for the problem. If Lagrangian elements are used the components of $\{u\}$ and $\{\rho\}$ are simply nodal values of the variables. If Hermitian elements are used they contain both nodal values and nodal derivatives. In the current model three noded quadratic Lagrangian elements and two noded cubic Hermitian elements are used. The Lagrangian elements are one-dimensional equivalents of the eight noded isoparametric rectangles of Ref. 12. Typical Lagrangian and Hermitian meshes showing "displacement" and "rotational" degrees of freedom are shown in Fig. 1.

Equations (5) may be written in matrix form as

$$\{\tilde{f}\} = \begin{Bmatrix} \tilde{u} \\ \tilde{\rho} \end{Bmatrix} = [N]\{\delta\} \quad (6)$$

where $\{\delta\}$ contains the components of $\{u\}$ and $\{\rho\}$. $[N]$ is formed from the appropriate components of $[N_g]$. If $\{\delta\}$ is suitably ordered, Eq. (6) may be partitioned to give

$$\{\tilde{f}\} = [N_i N_1 N_2] \begin{Bmatrix} \delta_i \\ \delta_1 \\ \delta_2 \end{Bmatrix} \quad (7)$$

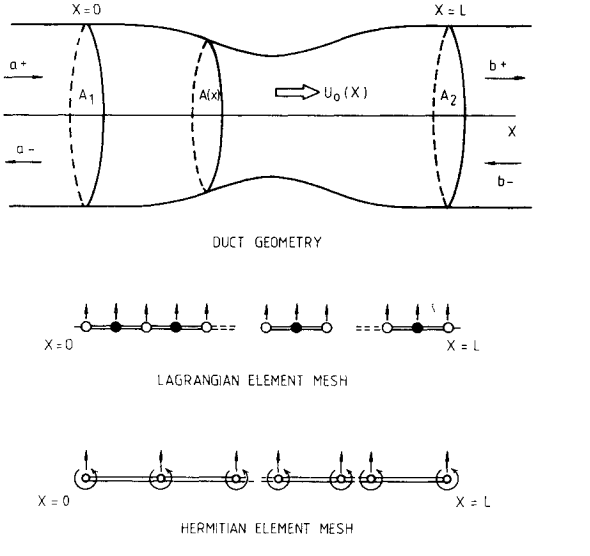


**Fig. 1 Duct geometry and FEM discretizations.**

where $\{\delta_i\}$ contains the internal degrees of freedom for the system, $\{\delta_1\}$ contains the degrees of freedom at $x=0$, and $\{\delta_2\}$ those at $x=L$. The trial function may now be modified to identically satisfy the modal decompositions at $x=0$ and $x=L$. If $a^+$ and $a^-$ are the modal coefficients at $x=0$ the values of $u$, $du/dx$, $\rho$ and $d\rho/dx$ at $x=0$ are given by

$$u(0)=c_0/\rho_0[a^+-a^-]$$

$$\theta(0)=\frac{du}{dx}\Big|_{(x=0)}=\frac{c_0}{\rho_0}[-ik^+a^++ik^-a^-]$$

$$\rho(0)=a^++a^-$$

$$\phi(0)=\frac{d\rho}{dx}\Big|_{(x=0)}=ik^+a^+-ik^-a^-$$

For the Lagrangian formulation $\{\delta_1\}$ may then be written

$$\{\delta_1\}=\begin{Bmatrix}u(0)\\ \rho(0)\end{Bmatrix}=\begin{bmatrix}c_0/\rho_0, & -c_0/\rho_0\\ 1, & 1\end{bmatrix}\begin{Bmatrix}a^+\\ a^-\end{Bmatrix}$$

The analogous expression for the Hermitian formulation is

$$\{\delta_1\}=\begin{Bmatrix}u(0)\\ \theta(0)\\ \rho(0)\\ \phi(0)\end{Bmatrix}=\begin{bmatrix}c_0/\rho_0 & -c_0/\rho_0\\ -ik^+c_0/\rho_0, & ik^-c_0/\rho_0\\ 1 & 1\\ -ik^+ & -ik^-\end{bmatrix}\begin{Bmatrix}a^+\\ a^-\end{Bmatrix}$$

In either event $\{\delta_1\}$ is given by

$$\{\delta_1\}=[T_1]\{a\}$$

where $\{a\}=[a^+, a^-]^T$. Similarly $\{\delta_2\}$ may be written

$$\{\delta_2\}=[T_2]\{b\}$$

where $\{b\}=[b^+, b^-]^T$, $b^+$ and $b^-$ denoting the positive and negative modal coefficients at $x=L$. Equation (7) may then be rewritten

$$\{\tilde{f}\}=[N_i\ N_1T_1\ N_2T_2]\begin{Bmatrix}\delta_i\\ a\\ b\end{Bmatrix}=[N']\{\Delta\} \tag{8}$$

In this form the trial function is an expansion for $\{\tilde{f}\}$ in terms of known basis functions (the components of $[N']$) and unknown coefficients (the components of $\{\Delta\}$). The unknown coefficients include both nodal degrees of freedom and modal coefficients at the upstream and downstream boundaries. It is useful to note at this stage that $[N']$ is given in terms of $[N]$ by the transformation

$$[N']=[N][T]\text{ where }[T]=\begin{bmatrix}I & 0 & 0\\ 0 & T_1 & 0\\ 0 & 0 & T_2\end{bmatrix} \tag{9}$$

**Formation and Minimization of Residuals**

Equations (1) and (2) may conveniently be written

$$[L]\begin{Bmatrix}u\\ \rho\end{Bmatrix}=\begin{Bmatrix}0\\ 0\end{Bmatrix} \tag{10}$$

where $[L]$ is a $2\times2$ linear matrix differential operator. When the trial function of Eq. (8) is substituted into Eq. (10) a residual $\{R\}$ is formed where

$$\{R\}=[L]\{\tilde{f}\}=\Big[[L][N']\Big]\{\Delta\} \tag{11}$$

$\{R\}$ must now be minimized over the region $0\le x\le L$. The Galerkin process and RLS method are used for this purpose.

The application of the Galerkin process orthogonalizes the residual with respect to the basis functions of the trial expansion. This procedure yields the equation

$$[K_G']\{\Delta\}=\{0\},\text{where}[K_G']=\int_0^L[N']^T\Big[[L][N']\Big]A\,dx \tag{12}$$

From Eq. (9) we observe that $[K_G']$ may also be written

$$[K_G']=[T]^T[K_G][T]\text{where }[K_G]=\int_0^L[N]^T\Big[[L][N]\Big]A\,dx \tag{13}$$

In this form the submatrices of $[K_G]$ may be assembled in the usual way from analogous element submatrices.

The RLS formulation proceeds from the minimization of the functional

$$\chi=\int_0^L\{R\}^{*T}\{R\}A\,dx$$

with respect to the free variables in the trial expansion. This yields the equation

$$[K_{LS}']\{\Delta\}=\{0\} \tag{14}$$

where

$$[K_{LS}']=\int_0^L\Big[[L][N']\Big]^{*T}\Big[[L][N']\Big]A\,dx$$

$[K_{LS}']$ may also be written

$$[K_{LS}']=[T]^{*T}[K_{LS}][T]$$

where

$$[K_{LS}]=\int_0^L\Big[[L][N]\Big]^{*T}\Big[[L][N]\Big]A\,dx$$

and assembled in this form from the appropriate element submatrices. Each row of Eq. (14) corresponds to minimization of $\chi$ with respect to a particular component $\{\Delta\}$, just as with the Galerkin process each row of Eq. (12) corresponds to orthogonalization with respect to the corresponding basis function. In specific solutions some components of $\{\Delta\}$ will be known (e.g., known incident modal coefficients at $x=0$) and these rows of Eqs. (12) and (14) must be deleted. A complete set of equations for the unknown modal coefficients and internal values of $u$ and $\rho$ then results.

The procedure just described although presented only for the one-dimensional case clearly may be applied to two- and three-dimensional problems by appropriate modification of the variables, operators, and shape functions. A complete treatment of the two-dimensional formulation, restricted to Lagrangian discretizations, is to be found in Ref. 12.

## Numerical Results

### General Comments

Two separate criteria arise in assessing the performance of the various FEM formulations. An important characteristic of any successful FEM application to realistic turbofan configurations is the efficient representation of high-frequency acoustical fields with many axial wavelength variations within the solution region. Initially, therefore, the performance of the FEM schemes is assessed in representing essentially harmonic-type axial variations of velocity and pressure. Uniform duct sections for which exact solutions are readily available are used for this purpose. The number of degrees of freedom required by each formulation to attain a specified order of accuracy for a given frequency and Mach number then becomes a significant measure of the computational efficiency of the scheme. It will be demonstrated that the Galerkin and RLS formulations with Hermitian elements are significantly and consistently more efficient in this regard than either of the Lagrangian formulations.

The second aspect of the performance of the FEM formulations addressed in this section relates to their behavior in nonuniform flows where the local Mach number and the associated convective terms in the acoustical equations vary with the cross section of the duct. The effects of such variations are particularly significant for high Mach number regimes where the local wavenumber of the disturbance is highly sensitive to small variations in sectional area. The relative efficiencies of the various schemes in converging to stable solutions independent of further mesh refinement for configurations of this sort are demonstrated by the presentation of results for a converging-diverging duct with a severe contraction ratio and a near sonic Mach number.

### Results for Uniform Ducts

For a uniform duct the positive and negative wavenumbers of Eq. (4) reduce to

$$k^{\pm} = k/(M \pm 1) \tag{15}$$

where $M$ is the Mach number of the mean flow. The pressure field along the duct with a positive mode incident at the left-hand end is then given by

$$P(x) = a^{+} e^{-ik^{+}x} \tag{16}$$

where $a^{+}$ is the amplitude of the incident mode. The resulting values the transmission coefficients, $b^{+}$ and $b^{-}$, are then $a^{+}\exp(ik^{+}L)$ and zero, respectively. For the results presented in this section a uniform duct of unit length is considered. Acoustical fields and modal coefficients are calculated for Mach numbers of 0.0, $-0.5$, and $-0.75$ with a reduced frequency, $k = 2\pi$. The computed results are then compared with the analytic solutions of Eqs. (15) and (16). For these parameters the solutions correspond to pressure variations of one, two, and four wavelengths along the duct. The normalized error $\epsilon$ in the computed transmission coefficient forms a convenient measure of the accuracy of each scheme. $\epsilon$ is defined by

$$\epsilon = \left| b^{+}/a^{+} - e^{ik^{+}L} \right| \tag{17}$$

where $a^{+}$ is the known incident coefficient, $b^{+}$ the computed transmission coefficient, and $k^{+}$ the exact wavenumber given by Eq. (15).

Some typical results for the transmission error are shown in Fig. 2 for the case $M = 0.0$. Values of $\epsilon$ are plotted on a logarithmic scale for the four FEM schemes. The ordinate is the number of degrees of freedom per variable (a direct measure of the dimension of the stiffness matrices $[K'_G]$ or $[K'_{LS}]$ of Eqs. (12) and (14)). It is immediately apparent from Fig. 2 that both of the Hermitian element formulations are significantly more accurate than their Lagrangian counterparts. This was found to hold for all Mach numbers and frequencies investigated. A second obvious characteristic of the results of Fig. 2 is the intersection of the Galerkin and RLS curves (for both the Hermitian and Lagrangian formulations) if the number of degrees of freedom is sufficiently large. This feature was not apparent in the two-dimensional Lagrangian studies of Ref. 12, where constraints on the number of degrees of freedom that could be used within acceptable limits of computational cost restricted the analysis to relatively coarse meshes. It was assumed incorrectly in these studies that the Lagrangian RLS scheme was inherently less accurate than the equivalent Galerkin scheme. This is clearly not the case since if a large enough number of degrees of freedom are used both the Lagrangian and Hermitian RLS schemes become more accurate than their Galerkin counterparts. This is of doubful practical significance since for "reasonable" practical errors, of the order of 1%, say, the Galerkin schemes remain the more efficient of the two residual formulations, though in the Hermitian case only marginally so.

It is reassuring to observe at this stage that the nature of the error in the one-dimensional RLS schemes closely resembles that already observed in the two-dimensional formulations. In both cases the acoustical field is numerically damped with increasing distance from the inlet plane. For comparison the axial pressure fields for the one-dimensional Hermitian, one-dimensional Lagrangian, and two-dimensional Lagrangian formulations are shown in Figs. 3-5 for a Mach number of $-0.5$. The axial resolution is similar in each case. The damping effect of the RLS formulations which is barely discernible in the Hermitian scheme (Fig. 3) is readily observable in both of the Lagrangian analyses (Figs. 4 and 5).

When values of $\epsilon$ are calculated for higher frequencies and Mach numbers the general features of Fig. 2 are preserved. A direct comparison of results for different frequencies and Mach numbers, however, requires a modification to the ordinate of Fig. 2. This is necessary to take into account the different numbers of axial wavelength variations within the solution region which will clearly affect the demands placed on the axial resolution of each scheme. This modification is achieved conveniently by plotting $\epsilon$ as a function of the number of degrees of freedom per variable per axial

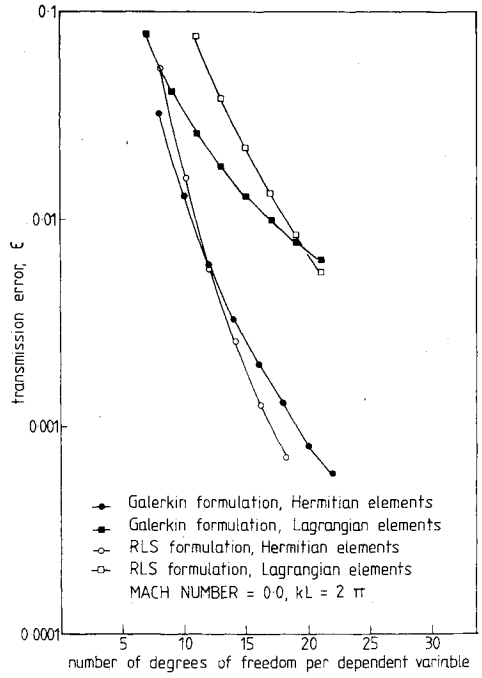


**Fig. 2 Transmission error for a uniform duct, $M = 0.0$, $kL = 2\pi$.**

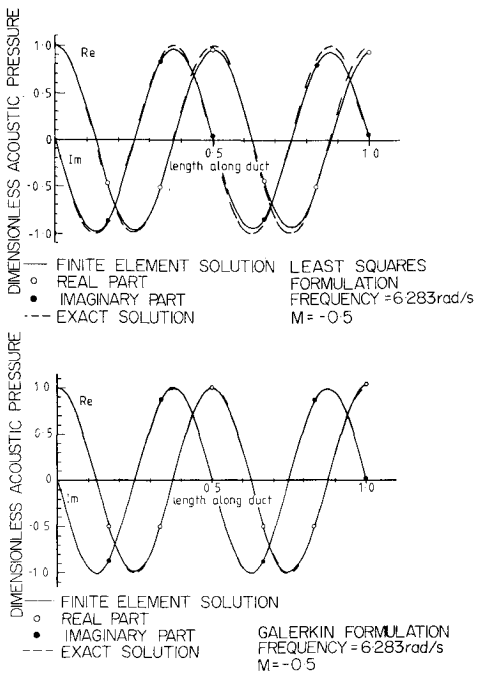


**Fig. 3 Axial pressure variation for a uniform duct, one-dimensional Hermitian element scheme.**

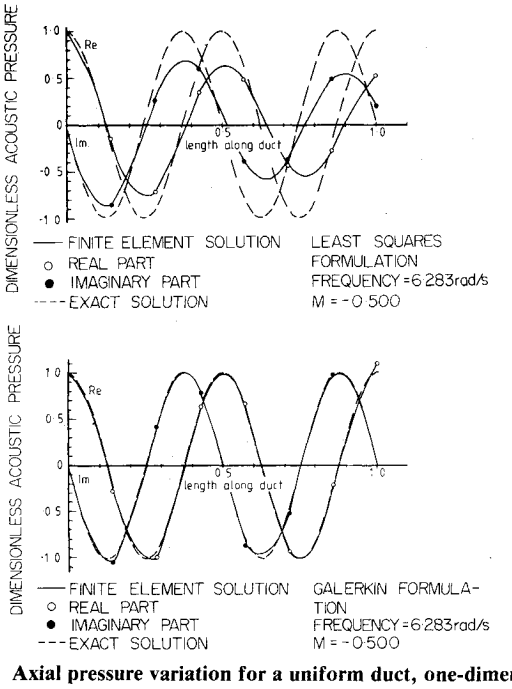


**Fig. 4 Axial pressure variation for a uniform duct, one-dimensional Lagrangian element scheme.**

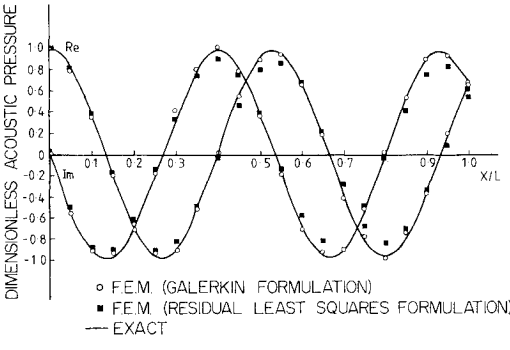


**Fig. 5 Axial pressure variation for a uniform duct, two-dimensional Lagrangian element scheme.**

wavelength variation in the resulting solution. If the frequency is held constant and the Mach number varied, or vice versa, this then permits direct comparison of errors for different numbers of wavelength variations along the duct. Comparisons of this sort are shown in Figs. 6 and 7 where results are presented separately for the Lagrangian (Fig. 6) and Hermitian (Fig. 7) formulations. In each case the frequency is held constant while values of $\epsilon$ are plotted for Mach numbers of 0.0, $-0.5$, and $-0.75$ corresponding to one, two, and four wavelength variations along the duct. A degeneration in accuracy as the adverse Mach number increases then indicates an undesirable trend toward cumulative errors in the numerical solution as the number of wavelengths in the solution region increases. A trend of this sort is readily observable in the Lagrangian RLS results of Fig. 6. This behavior effectively disqualifies the Lagrangian RLS scheme from serious consideration as a viable solution technique for the turbofan inlet problem. Cumulative errors of this sort do not occur for the other three formulations, all of which appear to give results relatively independent of Mach number. This is particularly true of the two Hermitian schemes which give results that lie within the narrow shaded band of Fig. 7, although a slight degradation of accuracy with increasing Mach number is observable for the Hermitian RLS formulation. Figures 6 and 7 are plotted to the same scale and a direct comparison of the two figures reinforces our previous supposition (from Fig. 2) that the use of Hermitian elements substantially improves the accuracy of either residual scheme. It can be seen that for a 1% error ($\epsilon = 0.01$), for example, the number of degrees of freedom per variable per wavelength required by the Hermitian formulations is approximately 10. For the Lagrangian-Galerkin formulation the analogous figure is in the region of 20 and for the Lagrangian-RLS formulation the figure is indeterminate. The disparity between Hermitian and Lagrangian results is exacerbated as higher accuracies are required. In view of their poor performance for the uniform case both of the Lagrangian schemes are omitted from serious consideration in the presentation of results for nonuniform ducts which follows. The Lagrangian RLS scheme is omitted altogether and the Lagrangian-Galerkin scheme is included only insofar as it establishes correspondence between the behavior of the one- and two-dimensional models.

### Numerical Results for Nonuniform Ducts

In this section results are presented for acoustical fields in nonuniform ducts. No analytic solutions are available for the nonuniform configurations considered and the accuracy of the FEM models is assessed by their convergence to stable solutions independent of further mesh refinement.

Most of the problems associated with nonuniform duct calculations stem from the widely disparate requirements placed on the axial resolution of the mesh at different stations of the duct. If the mean flow is relatively uniform the resolution requirements established in the preceding section for uniform ducts remain valid. For high Mach number regimes, however, or severe contractions of the sectional area, it is found that loss of local resolution may cause spatially unstable components to enter the Galerkin solutions and propagate throughout the solution region. The RLS formulations are not susceptible to this disorder but exhibit considerable numerical damping.

The preceding remarks are illustrated by the presentation of numerical results for a converging-diverging quartic duct with a severe contraction ratio of 0.5. This particular geometry corresponds to an experimental test duct for which a comparison of experimental and numerical results has recently been reported.[13] Numerical results are presented here for a reduced frequency, $kL = 2.16$, with an inlet Mach number of $-0.3$. The Mach number in the throat of the duct is then $-0.86$. The acoustical disturbance is amplified by the adverse mean flow and the effective wavenumbers [given by Eq. (15)]

are $k^+L=3$ and $k^+L=15$, respectively, at the inlet and throat. Clearly this is a computationally demanding problem with anticipated resolution requirements increasing by a factor of five within the solution region.

A series of two-dimensional Lagrangian-Galerkin axial pressure fields for this configuration are shown in Fig. 8. Of particular interest is the shape of the pressure field for a coarse $4\times8$ mesh (the description $4\times8$ denotes a mesh with 4 and 8 elements uniformly spaced across and along the duct, respectively). It can be seen that the solution is characterized by spatial oscillations within each element. It was behavior of this type in the two-dimensional and axisymmetric models that prompted the development of the one-dimensional model and suggested further numerical studies with higher-order elements. For comparison analogous one-dimensional Lagrangian-Galerkin solutions for the same problem are shown in Fig. 9. It can be seen that the same type of spatial instabilities are present in the one-dimensional formulation.

The oscillatory components in the preceding solutions result in severe slope discontinuities at element boundaries. When Hermitian elements are used, which preclude such behavior by virtue of their intrinsic $C_1$ continuity, spatial instabilities again manifest themselves, this time in the form of smoothly oscillatory components. Behavior of this sort is shown in Fig. 10 where Hermitian-Galerkin solutions are plotted for the same problem. For both the Lagrangian and Hermitian formulations the oscillatory components in the solution disappear if the total number of elements is sufficiently large. It is clear that this problem arises not from any overall inadequacy of the mesh but from the high demands placed on its resolution in the close vicinity of the throat. This is demonstrated in Fig. 11 where Hermitian-Galerkin results are presented for axially modified meshes with the same total number of elements as in Fig. 10 but with smaller elements placed near the throat. A dramatic increase in the rate of convergence of the solutions is then realized. This effect applies also to the Lagrangian-Galerkin solutions as demonstrated by the axially modified mesh results included in the two-dimensional results of Fig. 8.

The spatial instabilities which characterize the Galerkin formulations do not occur in the analogous RLS schemes. The RLS solutions are always smooth and loss of resolution is indicated by an artificially damped solution. A sequence of Hermitian RLS solutions for the same configuration is presented in Fig. 12. Once again mesh modification is an effective means of increasing the convergence of the scheme. This is illustrated by a comparison of Figs. 12 and 13 showing RLS solutions for uniform and modified meshes.

A quantitative measure of the effect of axial mesh modification is presented in Fig. 14 which shows the error from their final converged values of the transmission and reflection coefficients $b^+$ and $a^-$ for uniform and modified meshes. The ordinate in this case is the number of axial elements. It can be seen that large increases in the accuracy, and, hence, computational efficiency, of both the Galerkin and RLS schemes result from the modification of the mesh. The results for Fig. 14 are computed for the Hermitian formulations and correspond to the pressure fields of Figs.

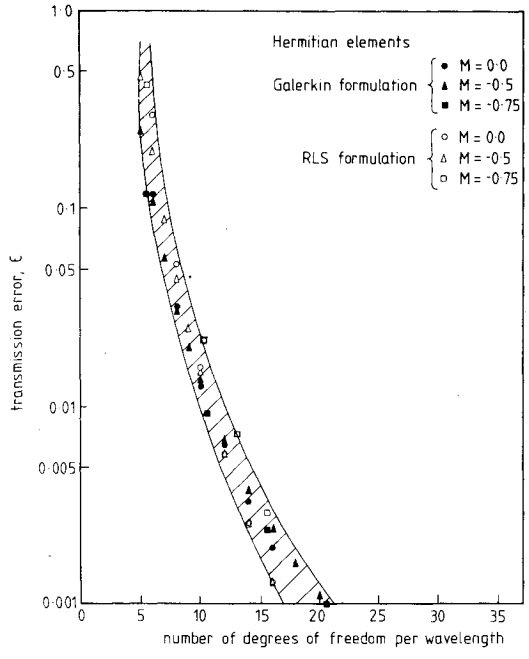


**Fig. 7 Transmission error for a uniform duct, Hermitian element scheme.**

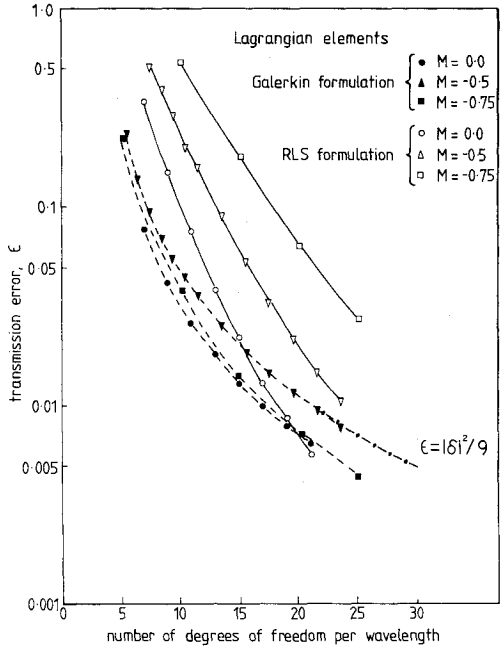


**Fig. 6 Transmission error for a uniform duct, Lagrangian element scheme.**

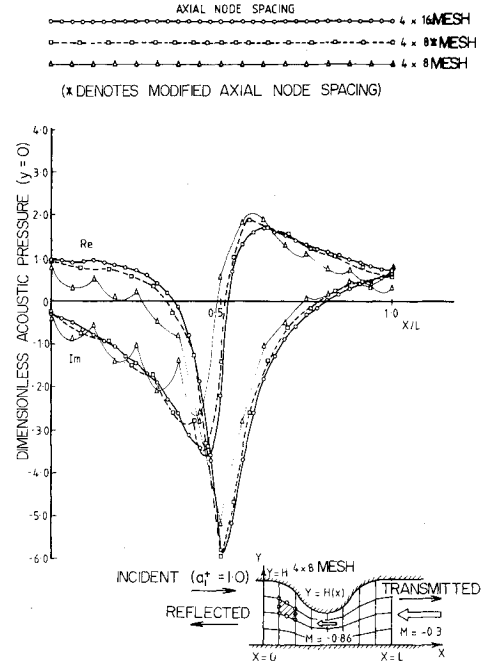


**Fig. 8 Axial pressure for a nonuniform duct, two-dimensional Lagrangian-Galerkin scheme.**

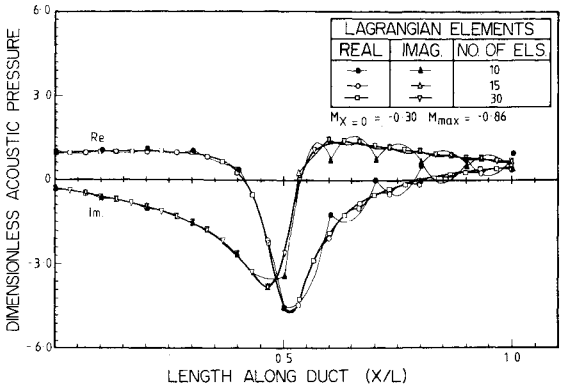


**Fig. 9 Axial pressure for a nonuniform duct, one-dimensional Lagrangian-Galerkin scheme.**

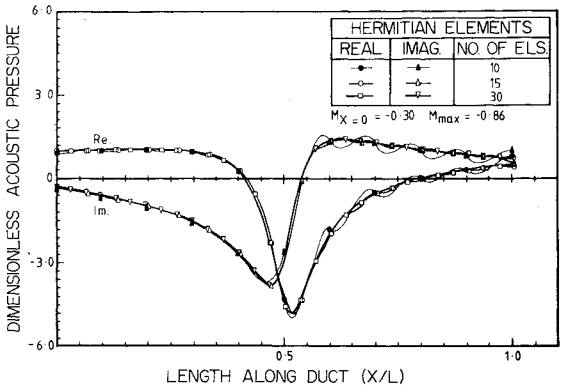


**Fig. 10 Axial pressure for a nonuniform duct, one-dimensional Hermitian-Galerkin scheme, uniform mesh.**

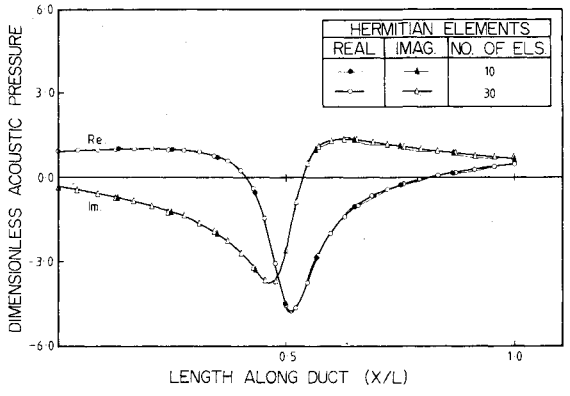


**Fig. 11 Axial pressure for nonuniform duct, one-dimensional Hermitian-Galerkin scheme, modified mesh.**

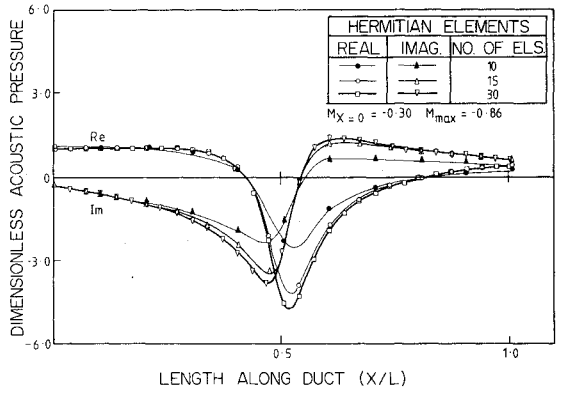


**Fig. 12 Axial pressure for a nonuniform duct, one-dimensional Hermitian RLS scheme, uniform mesh.**

10-13. The mesh spacing algorithm is by no means optimal but serves to indicate that the FEM models may be greatly enhanced even by relatively crude adjustments to the mesh. Clearly for the more costly two- and three-dimensional models considerable thought should be given to optimizing this procedure. It is worth observing at this point that in related studies of the duct eigenvalue problem[10] the variation of mesh spacing in the transverse direction was also shown to be effective in improving the accuracy of the resulting solutions. The ease with which finite element models can accommodate compatible elements of varying sizes without modification to the general computational scheme constitutes a significant advantage over alternative numerical techniques which might be applied to this problem.

## Analytic Considerations

### Difference Solutions of the Steady Problem

For a uniform duct with nodes spaced an equal distance $\Delta x$ apart the scalar equations forming the rows of Eqs. (12) and (14) have the same form for all nodes of the same type. A general difference solution may then be obtained for the nodal variables. The formation and solution of the difference equations in this way involves considerable algebraic manipulation but is conceptually straightforward. The procedure is already well established in other areas of FEM

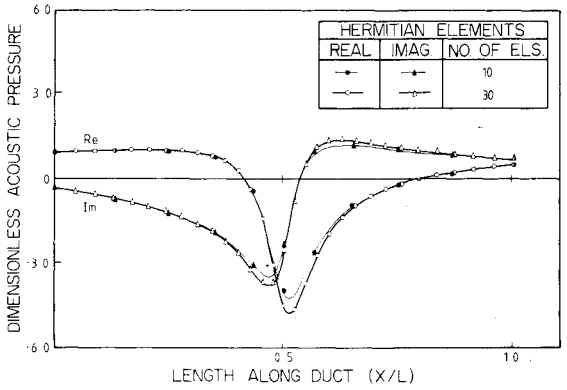


**Fig. 13 Axial pressure for a nonuniform duct, one-dimensional Hermitian RLS scheme, modified mesh.**

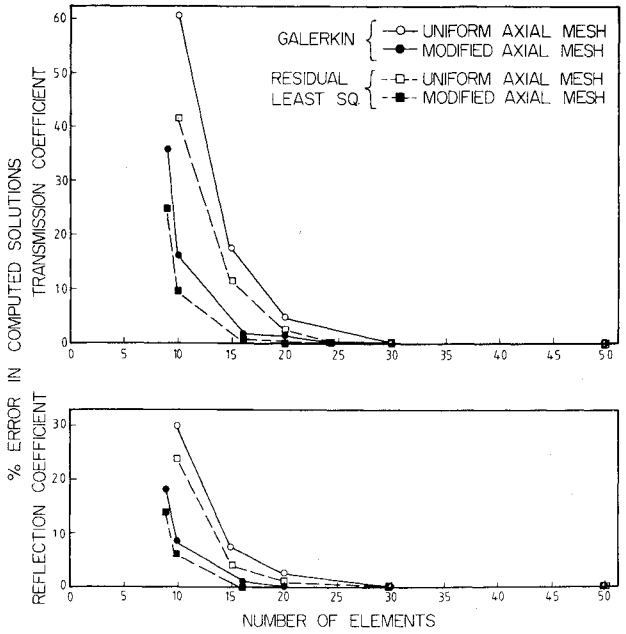


**Fig. 14 Error in transmission and reflection coefficients for the nonuniform case, Hermitian element schemes.**

application[15] as a means of investigating the general characteristics of the resulting numerical solutions. The details of this analysis for the current problem will be omitted and only the results reported.

For the Galerkin-Lagrangian scheme with quadratic elements the general form of the difference solution at interelement nodes is

$$\rho_m = A_1^+ \kappa_1^{+m} + A_2^+ \kappa_2^{+m} + A_1^- \kappa_1^{-m} + A_2^- \kappa_2^{-m}$$

$$u_m = A_1^+ \kappa_1^{+m} + A_2^+ \kappa_2^{+m} - A_1^- \kappa_1^{-m} + A_2^- \kappa_2^{-m} \tag{18}$$

where $\rho_m$ and $u_m$ denote the nodal values of $\rho$ and $u$ at interelement node $m$ (see Fig. 16a). $A_{1,2}^{\pm}$ are arbitrary constants to be fixed by the boundary conditions and $\kappa_{1,2}^{\pm}$ are the roots of

$$\kappa^2(5+4\delta+\delta^2) - \kappa(10+6\delta^2) + (5-4\delta+\delta^2) = 0 \tag{19}$$

The form of the solution for the analogous RLS formulation is identical to that of Eq. (18) except that $\kappa_{1,2}^{\pm}$ are now given by the roots of

$$\kappa^2[(10-4\delta^2)(\delta^2+5\delta+5/2) - (\delta^2+10\delta+10)^2]$$

$$+\kappa[(10-4\delta^2)(35-8\delta^2) - 2(\delta^2+10)^2 + 200\delta^2]$$

$$+[(10-4\delta^2)(\delta^2-5\delta+5/2) - (\delta^2-10\delta+10)^2] = 0 \tag{20}$$

The parameter $\delta$ in both cases is given by $\delta = \delta^+ = ik^+\Delta x$ for the $\kappa^+$ roots and $\delta = \delta^- = ik^-\Delta x$ for the $\kappa^-$ roots, where $k^{\pm}$ are the exact wavenumbers for positive and negative exact solutions as defined in Eq. (15) of the preceding section.

The exact solution of the original equations may be written in the general form

$$\rho = A^+ e^{-ik^+x} + A^- e^{-ik^-x}$$

$$\rho = A^+ e^{-ik^+x} - A^- e^{-ik^-x} \tag{21}$$

where the first and second terms represent positive and negative modes and the constants $A^+$ and $A^-$ are determined by the boundary conditons at $x=0$ and $x=L$. At nodal points Eq. (21) may be rewritten

$$\rho_m = A^+ \kappa_E^{+m} + A^- \kappa_E^{-m} \qquad u_m = A^+ \kappa_E^{+m} - A^- \kappa_E^{-m} \tag{22}$$

where

$$\kappa_E^{\pm} = e^{-ik^{\pm}(2\Delta x)} = e^{-2\delta^{\pm}}$$

A comparison of Eqs. (18) and (22) now reveals that for both the numerical and exact solutions the positive and negative modes are uncoupled, i.e., the $A^+$ terms in the difference solution correspond to the $A^+$ term in the exact solution in that in both cases the density and velocity are in phase. Similarly the $A^-$ terms in both solutions correspond to out of phase negatively propagating nodes. In addition, the positive and negative components of both the exact and the difference solutions depend only on the appropriate positive and negative wavenumbers $k^+$ and $k^-$, respectively. The uncoupling of the numerical solution in this manner is a property of the coupled first-order equations and does not arise if a single second-order Helmholtz-type formulation is used as the basis of the numerical scheme. Of more practical interest is the presence of two difference solutions for each positive or negative component of the exact solution, i.e., we note that either of the first two terms in Eq. (18) might correspond to the positive wave in the exact solution and similarly either of the last two terms in Eq. (18) is a candidate for representing the negative wave. It is clear that the extent to which either or both of the roots $\kappa_1$ and $\kappa_2$ correspond to $\kappa_E$ governs the degree to which the numerical solution can accurately represent the exact result. A comparison of exact and numerical values of $\kappa$ is presented in Fig. 15 where the real and imaginary parts of $\kappa_1$ and $\kappa_2$ [given by the solution of Eqs. (19) and (20)] are plotted against $\delta/i\pi$, $(=k^{\pm}\Delta x/\pi)$. The exact value $\kappa_E$ of Eq. (22) is also plotted. The ordinate $\delta/i\pi$ has the physical significance that a value of 1.0 corresponds to a nodal spacing equivalent to one element per wavelength. It can be seen that the $\kappa_1$ Galerkin root is a good approximation to the exact solution for values of $\delta/i\pi$ as large as 0.5 (two elements per wavelength). The $\kappa_2$ root, however, bears little resemblance to the exact solution except insofar as it converges to the exact value of unity as $\delta \to 0$. The characteristics of the RLS roots are quite different with both roots showing a reasonable correspondence to the exact value although neither of them is as accurate as the $\kappa_1$ Galerkin root. Asymptotically the Galerkin scheme gives

$$\kappa_1 = \kappa_E + \text{terms of order } \delta^5$$

$$\kappa_2 = \kappa_E + \text{terms of order } \delta \tag{23}$$

For the RLS scheme, however,

$$\kappa_{1,2} = \kappa_E + \text{terms of order } \delta^3 \tag{24}$$

From Eq. (23) we may deduce that if it were possible to represent the solution entirely in terms of the $\kappa_1$ components of the Galerkin solution the error involved would be of order $\delta^4$. Clearly, this is not the case since from Figs. 2 and 6 (whose ordinate is proportional to the inverse of $\delta$) we can demonstrate that the error in the Lagrangian-Galerkin solution varies very nearly as $\delta^2$. This apparent discrepancy between the numerical and analytical studies arises from the inevitable presence of a component of the $\kappa_2$ solution when boundary conditions are imposed at the duct terminations. This effect dominates the accuracy of the Galerkin solution. If the appropriate difference equations are formed for nodes at $x=0$ and $x=L$ the relationship between the $\kappa_1$ and $\kappa_2$ contributions may be obtained. For a uniform duct with the same anechoic boundary conditions as already imposed on the numerical scheme the constants $A_1^+$ and $A_2^+$ are related by $A_2^+ = \beta A_1^+$ where $\beta \sim \delta^2/18$ for the Galerkin solution and $\beta \sim \frac{1}{2}$ for the RLS solution. For the Galerkin solution this enables us to form an asymptotic upper bound for the transmission error of Figs. 2 and 6 as $\delta \to 0$. After some manipulation it can be shown that

$$|\epsilon| \leq |\delta|^2/9 \text{ as } |\delta| \to 0 \tag{25}$$

This estimate is plotted on Fig. 6 and closely corresponds to the maximum calculated numerical values of $\epsilon$ as the number of degrees of freedom per variable per wavelength becomes large. Since Eq. (25) is independent of frequency and Mach number, except insofar as they occur in the expression for $\delta$, the existence of an upper limit of this sort confirms our previous assertion from the numerical studies that no cumulative errors appear in the Galerkin formulations with increasing frequency or Mach number. The authors have been unable to derive any such upper bound for the RLS formulation and indeed the numerical results would appear to suggest that no such limit exists.

It might be assumed that the presence of two numerical roots $\kappa_1$ and $\kappa_2$ for each exact mode is a function of the element topology. This is not the case. It is not difficult to show that whatever type of Lagrangian elements are used the general form of Eq. (18) is preserved. It is an inevitable consequence of the formulation of the problem in terms of coupled first-order equations that spurious numerical components will be generated.

The preceding statement throws considerable light on the characteristics of the nonuniform duct solutions of the

preceding section when the shape of the $\kappa_1$ and $\kappa_2$ components are investigated. To do this it is necessary to obtain expressions for the variables at a typical midside node, denoted by node $m + \frac{1}{2}$ in Fig. 16a. The solution at such nodes is given by expressions for $u$ and $\rho$ similar to those of Eq. (18) but with the $A$'s replaced by $B$'s. The $A$'s and $B$'s are not independent but related by

$$B_i^{\pm} = \alpha_i^{\pm} A_i^{\pm}, \qquad i = 1,2$$

where the factors $\alpha$ are derived as part of the eigenvalue process leading to Eqs. (19) and (20). In the limit as $\delta \to 0$ it can be shown that

$$\alpha_1^{+} \to +1 \text{ and } \alpha_2^{+} \to -\tfrac{1}{2} \tag{26}$$

for the Galerkin scheme and $\alpha_{1,2}^{+} \to +1$ for the RLS scheme.

The cases $\alpha \to 1.0$ represent a smooth solution, i.e., the values of the nodal variables at adjacent nodes are equal. The case $\alpha \to -\frac{1}{2}$ however represents a component of the solution that changes sign at each node and is of the shape shown in Fig. 16a. The existence of such a component only in the Galerkin formulation and not in the RLS scheme [see Eqs. (26)] clearly correspond to the existence of the cusped

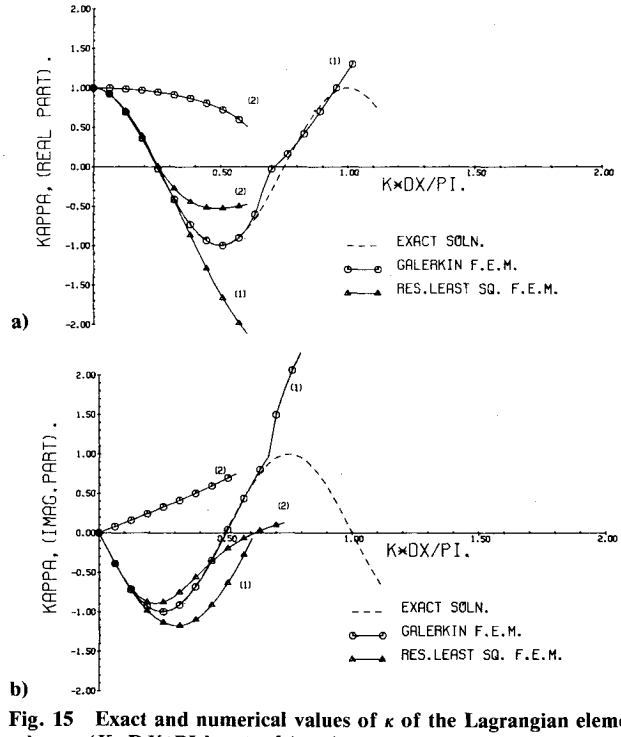


**Fig. 15 Exact and numerical values of $\kappa$ of the Lagrangian element schemes ($K_*$ DX/PI denotes $k\Delta x/\pi$).**

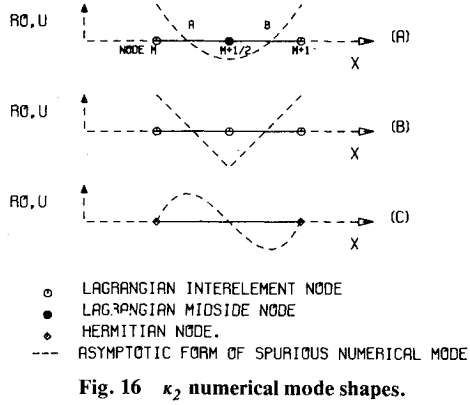


**Fig. 16 $\kappa_2$ numerical mode shapes.**

solutions evident in the Galerkin results of the previous section. It is not difficult to show that similar modes exist for higher- and lower-order elements. For example, if linear elements are used the equivalent component has the form shown in Fig. 16b. "Sawtooth" solutions of this sort have been observed in Abrahamson's solutions with quasilinear elements.[7] With difficulty the analysis already described for Lagrangian elements may be repeated for the Hermitian elements of the current model. The authors have performed such an analysis to the extent of demonstrating the existence in the Hermitian-Galerkin scheme of asymptotic components of the form shown in Fig. 16c.

Returning to the Lagrangian quadratic elements it is of interest to note that the points at which the spurious components of the solution are zero correspond to the reduced integration points for the element. In Fig. 16a, for example, the points A and B are the Gauss integration points for a two point integration scheme, one point less than would be required for exact evaluation of the element stiffness matrix. Sampling the solution at reduced integration points, as practiced in other finite-element applications, would certainly improve the appearance of the resulting solutions but would not affect the accuracy of the results as measured, for example, by the transmission error plotted in Figs. 2, 6, and 7.

In conclusion, the analytic difference solutions tend to confirm the conclusions indicated by the numerical studies of the preceding section. They reveal that an inevitable result of the Galerkin formulation is the generation of nonphysical modes which dominate the accuracy of the method and are excited by inadequate resolution in the nonuniform case. The existence of such modes is independent of the type of element used. The RLS schemes do not generate such components and, hence, produce smooth but not necessarily more accurate solutions since the error in the Galerkin schemes is at least bounded irrespective of the number of wavelengths present. No such property appears to hold for the RLS schemes.

## Conclusions

The following conclusions are drawn from the preceding numerical and analytic studies.

1) Of the four schemes considered, the Hermitian-Galerkin formulation appears to be the most suitable scheme for further full-scale implementation. The Hermitian RLS scheme, although comparable in accuracy for the cases considered in this paper, exhibits a tendency to cumulative errors which mitigates against its use for high-frequency configurations.

2) The performance of both of the Lagrangian element schemes compares poorly with that of their Hermitian element counterparts. This is particularly true of the Lagrangian RLS scheme.

3) The presence of internal oscillatory components is an inevitable consequence of the Galerkin formulation irrespective of element type. The solutions produced by such schemes may be enhanced by ensuring adequate resolution of all points in the mesh. For nonuniform high Mach number flows this involves careful adjustment of the axial element spacing.

## Acknowledgments

The research program reported here has been supported by the NASA Lewis Research Center under Grant NSG-3231.

## References

[1] Craggs, A., "A Finite Element Method for Damped Acoustic Systems; An Application to Evaluate the Performance of Reactive Mufflers," *Journal of Sound and Vibration*, Vol. 48, 1976, pp. 377-392.

[2] Watson, W. R., "A Finite Element Simulation of Sound Attenuation in a Finite Duct with Peripherally Variable Liner," NASA TMS-74080, 1977.

[3]Kagawa, Y., Yamabuchi, T., and Mori, A., "Finite Element Simulation of an Axisymmetric Acoustic Transmission System with a Sound Absorbing Wall," *Journal of Sound and Vibration,* Vol. 53, 1977, pp. 357-374.

[4]Astley, R. J. and Eversman, W., "A Finite Element Method for Transmission in Nonuniform Ducts Without Flow: A Comparison with the Method of Weighted Residuals," *Journal of Sound and Vibration,* Vol. 57, 1978, pp. 367-388.

[5]Sigman, R. K., Majjigi, R. K., and Zinn, B. T., "Use of Finite Element Techniques in the Determination of the Acoustical Properties of Turbofan Inlets," AIAA Paper 77-18, 1977.

[6]Abrahamson, A. L., "A Finite Element Formulation for Sound Propagation in Ducts Containing Compressible Mean Flow," AIAA Paper 77-1301, 1977.

[7]Astley, R. J. and Eversman, W., "A Finite Element Formulation of the Eigenvalue Problem in Lined Ducts with Flow," *Journal of Sound and Vibration,* Vol. 65, 1979, pp. 61-74.

[8]Quinn, D. W., "A Finite Element for Computing Sound Propagation in Ducts Containing Flow," AIAA Paper 79-0661, 1979.

[9]Kagawa, Y., Yamabuchi, T., Yoshikawa, T., Ooie, S., and Kyouno, N., "Finite Element Approach to Acoustic Transmission-Radiation Systems and Applications to Horn and Silencer Design," *Journal of Sound and Vibration,* Vol. 69, 1980, pp. 207-228.

[10]Astley, R. J. and Eversman, W., "The Finite Element Duct Eigenvalue Problem: An Improved Formulation with Hermitian Elements and No Flow Condensation," *Journal of Sound and Vibration,* Vol. 69, 1980, pp. 13-25.

[11]Astley, R. J., Walkington, N. W., and Eversman, W., "Transmission in Flow Ducts with Peripherally Varying Linings," AIAA Paper 80-1015, 1980.

[12]Astley, R. J. and Eversman, W., "Acoustic Transmission in Lined Ducts with Flow, Part 2: The Finite Element Method," *Journal of Sound and Vibration,* Vol. 74, 1981, pp. 103-121.

[13]Baumeister, K. J., Eversman, W., Astley, R. J., and White, J. W., "Application of Steady State Finite Element and Transient Finite Difference Theory to Sound Propagation in a Variable Area Duct: A Comparison with Experiment," AIAA Paper 81-2017, 1981.

[14]Labrujere, T., DeVries, G., and Norrie, D. H., "A Least Squares Finite Element Solution for Potential Flow," Univ. of Calgary, Dept. of Mechanical Engineering, Rept. 86, 1976.

[15]Christie, I., Griffiths, D. F., Mitchell, A. R., and Zienkiewicz, O. C., "Finite Element Methods for Second Order Differential Equations with Significant First Derivatives," *International Journal for Numerical Methods in Engineering,* Vol. 10, 1976, pp. 1389-1396.